Kinetics and Thermodynamics of Dimer Formation and Dissociation for a Recombinant Humanized Monoclonal Antibody to Vascular Endothelial Growth Factor

Jamie M. R. Moore,‡ Thomas W. Patapoff, and Mary E. M. Cromwell*

Department of Pharmaceutical R&D, Genentech, Inc., 1 DNA Way, South San Francisco, California 94080

Received March 9, 1999; Revised Manuscript Received July 27, 1999

ABSTRACT: The recombinant humanized antibody (rhuMAb) VEGF has a high affinity for vascular endothelial growth factor and is currently being evaluated in clinical trials as a cancer therapeutic. Under acidic pH and low ionic strength conditions, the antibody was predominantly present as monomer. Under physiological conditions, the appearance of significant amounts of a noncovalent, reversible dimer were observed by size-exclusion chromatography. The kinetics and thermodynamics of the reversible self-association for rhuMAb VEGF monomer were investigated as a function of pH, temperature, and ionic strength by size-exclusion chromatography using the concentration jump method. The rate constant for dimer formation ranged 23−112 M^{-1} min^{-1} under the conditions studied, values that are significantly lower than those reported in the literature for other proteins that self-associate. The rate constant for dissociation ranged 0.0039−0.021 min^{-1}. Gibbs' free energies, enthalpies, entropies, and activation energies were determined and revealed that dimer formation is optimal at pH 7.5−8.0, which may be reflective of charge shielding occurring near the pI of the protein. There was a negative change in entropy for dissociation (values from −18.1 to −12.8 cal/mol K). In the presence of D_2O or 1 M NaCl, dimerization was enhanced. The results of the kinetic and thermodynamic analysis of this study indicate that rhuMAb VEGF dimerization occurs primarily through hydrophobic interactions.

There are many documented cases of proteins that reversibly self-associate in aqueous conditions. The dimerization of α-chymotrypsin, for example, has been studied by measuring thermodynamic parameters as a function of pH and ionic strength (*1*, *2*). The effect of pH led to the discovery of a direct interaction between the imidazole of a histidine and the α-carboxyl of a tyrosine between monomers. The enhancement of dimerization at high ionic strength resulted from the displacement of water from hydrophobic regions and charged groups in the contact region.

Immunoglobulin self-association has not been as extensively studied. One group of antibodies known to reversibly self-associate are cryoglobulins. The aggregation of these serum immunoglobulins have been linked to the pathophysiology of certain diseases such as rheumatoid arthritis (*3*) and idiopathic cryoglobulinemia (*4*). Self-association of IgG1-l myeloma protein is due to weak nonionic and hydrophobic interactions (*5*). Other cryoglobulins, specifically IgG3, self-associate via an interaction between glycosylated residues and other residues in the CH2 and CH3 domains (*6*).

This paper further explores the self-association of antibodies by studying the kinetics and thermodynamics of rhuMAb VEGF[1] self-association. RhuMAb VEGF is a member of the class of new therapeutics being investigated for their inhibition of angiogenesis. A humanized monoclonal antibody to vascular endothelial growth factor, rhuMAb VEGF, has been shown to suppress tumor growth in animal models by inhibiting VEGF-induced angiogenesis (*7*−*10*) and is currently being studied in clinical trials for the treatment of several solid tumor cancers.

The reversible aggregate of rhuMAb VEGF was discovered during its development for clinical studies. At pH 5.5 and below, rhuMAb VEGF existed predominately as a monomer as determined by size-exclusion chromatography. As pH, temperature, and ionic strength were raised, however, the protein formed aggregates. The aggregate was noncovalent and reverted back to monomer upon dilution. Other genetically engineered antibodies with the identical IgG1 framework as rhuMAb VEGF, such as trastuzumab and rituximab, do not form reversible dimer. This appears to be a unique characteristic of rhuMAb VEGF.

To understand the interactions responsible for rhuMAb VEGF self-association, kinetic and thermodynamic analyses were performed as a function of pH and ionic strength. This study explored the pH range 6.5−8.5. The ratio of dimer to monomer was monitored using size-exclusion chromatography. The rates of association and dissociation were determined at three temperatures. The dissociation equilibrium constant was calculated at a range of temperatures, 15−40 °C, enabling determination of $\Delta G°$, $\Delta H°$, and $\Delta S°$. The

* To whom correspondence should be addressed. Phone: (650) 225-1955. Fax: (650) 225-7203. E-mail: cromwell@gene.com.

‡ Current address, Department of Biopharmaceutical Sciences, University of California San Francisco, San Francisco, CA 94143.

[1] Abbreviations: VEGF, vascular endothelial growth factor; rhuMAb VEGF, recombinant humanized monoclonal antibody to VEGF; CHO, Chinese hamster ovarian; SEC, size-exclusion chromatography; pI, isoelectric point; K_D, dissociation equilibrium constant.

10.1021/bi9905516 CCC: $18.00
Published on Web 09/28/1999

effects of added NaCl and $CaCl_2$ were examined. Results obtained from this study contribute to the understanding of antibody self-association and will help develop a safe product for clinical studies.

EXPERIMENTAL PROCEDURES

Recombinant humanized anti-VEGF was purified to homogeneity from Chinese hamster ovarian (CHO) cells (*11*). Purified protein was dialyzed exhaustively against the desired buffer conditions at 5 °C. The following buffers were used: 10 mM Tris, pH 8.5, ± 1 M NaCl; 10 mM sodium phosphate, pH 7.5, ± 1 M NaCl; 10 mM Tris, pH 7.5, ± 1 M NaCl; 10 mM histidine, pH 6.5, ± 1 M NaCl; 10 mM sodium phosphate, pH 8.5, 8.0, 7.5, 7.0, and 6.5; 10 mM histidine, pH 5.5. The effect of ionic strength was explored further using 10 mM Tris, pH 7.5, with the addition of the following salts: 0−500 mM $CaCl_2$ and 0−1 M NaCl. The pH of the buffers was adjusted after all the components were added.

Dissociation Experiments. For dissociation experiments, the protein was concentrated to 30 mg/mL with a Centriprep 30 (Amicon). After concentration, the protein was filtered through a 0.22 μm membrane and stored at 40 °C for 72−96 h to increase the amount of dimer in the sample. The initiation of the dissociation experiments was performed by diluting the protein to 1 mg/mL using the same buffer. An aliquot was taken immediately and placed at 5 °C for the initial time point. The protein solutions were dispensed into polypropylene tubes and stored at 15, 30, and 40 °C. Samples were taken over time and stored immediately at 5 °C until analysis.

Equilibrium Experiments. The protein was concentrated to 30 mg/mL with Centriprep 30 cells (Amicon). The protein was then sterile filtered and stored at 40 °C for 72−96 h to accelerate dimer formation. The initiation of reequilibration was performed by diluting the protein to 1 mg/mL using the same buffer. This sample preparation was used for all protein solutions to maintain consistency. The protein solutions were dispensed into sterile polypropylene tubes and stored at 5, 15, 20, 25, 30, 35, and 40 °C. Samples were pulled at specified timepoints to ensure equilibrium was attained.

SEC. Size-exclusion chromatography (SEC) was used to analyze the amount of monomer and dimer present in the protein samples. Analysis was performed on an HP 1090M HPLC (Hewlett-Packard) using the HP ChemStation software. A TSK G3000SW_{XL} column (TosoHaas) at ambient temperature was used. The mobile phase was 10 mM phosphate and 1.15 M sodium chloride, pH 7.4. An isocratic gradient was utilized with a 1 mL/min flow rate for 15 min. The injection volume was 10 μL with detection at 214 and 280 nm. Data were reported as percent of total area of all protein-related peaks. The concentration of each species was determined by

$$\text{concentration (M)} = \frac{(\%\ \text{peak area})[\text{total protein concentrated (mg/mL)}]}{(M_r)\ (100)} \quad (1)$$

with $M_{monomer} = 150$ kDa and $M_{dimer} = 300$ kDa. The total protein concentration was determined by UV absorbance at 280 nm using an absorptivity of 1.7 cm mL/mg. The total area of the chromatograms was monitored to ensure mass balance.

Multiangle Light Scattering. To confirm the molecular mass of the aggregate species, a multiangle light scattering experiment was performed using an on-line miniDAWN light-scattering detector (Wyatt Technology) attached to the outlet of the SEC column on the HPLC. A refractive index detector was placed after the miniDAWN detector to determine the relative protein concentration in each peak. Using the SEC method described above, the individual peaks on the chromatogram were analyzed for molecular mass using Astra software (Wyatt Technology). The weight average molecular mass was determined for each peak with a Debye plot using the Zimm equation (*12*). The distribution of molecular mass did not vary over each peak studied in this experiment.

Determination of the Observed Rate Constant (k_{obs}). Assuming first-order kinetics for the dissociation reaction, the observed rate constant for the dissociation of dimer to monomer, k_{obs}, was determined from a plot of the concentration of dimer (D) vs time (t), which was fit using Kaleidagraph (Synergy Software) with the following equation

$$[D]_t = [D]_{eq} + ([D]_0 - [D]_{eq})\exp(-k_{obs}t) \quad (2)$$

where $[D]_t$ is the concentration of dimer at time t, $[D]_{eq}$ is the equilibrium concentration of dimer, and $[D]_0$ is the initial concentration of dimer. The error associated with the fit of the data was typically 5−20%. The experiment-to-experiment variability in the determination of the rate constants was approximately 25%.

Calculation of k_{assoc} and k_{dissoc}. A general treatment may be undertaken to determine the rate constant for reactions that are higher than first order for small perturbations from equilibrium which follow first-order kinetics. For an elementary reaction of the form

$$aA + bB \underset{k_r}{\overset{k_f}{\rightleftharpoons}} cC + eE \quad (3)$$

which follows the rate law,

$$-d[A]/(a\ dt) = k_f [A]^a[B]^b - k_r[C]^c[E]^e \quad (4)$$

and the observed rate constant, k_{obs}, is given by (*13*)

$$k_{obs} = k_f[A]_{eq}{}^a[B]_{eq}{}^b(a^2/[A]_{eq} + b^2/[B]_{eq}) + k_r[C]_{eq}{}^c[E]_{eq}{}^e(e^2/[E]_{eq} + c^2/[C]_{eq}) \quad (5)$$

For the reaction studied here,

$$2M \underset{k_{dissoc}}{\overset{k_{assoc}}{\rightleftharpoons}} D \quad (6)$$

eq 3 may be rewritten by letting A represent the monomer (M), C represent the dimer (D), $k_f = k_{assoc}$, and $k_r = k_{dissoc}$. Substituting the stoichiometric amounts, $a = 2$, $b = 0$, $c = 1$, and $e = 0$, into eq 3 reduces eq 5 to

$$k_{obs} = 4k_{assoc}[M]_{eq} + k_{dissoc} \quad (7)$$

Because there are two unknowns in this equation (k_{assoc} and k_{dissoc}) for any single concentration of $[M]_{eq}$, the equation for the equilibrium constant may be used to solve for the second unknown. The dissociation equilibrium constant, K_D, is given by

$$K_D = \frac{[M]_{eq}^2(\gamma_M)}{[D]_{eq}(\gamma_D)} = \frac{[M]_{eq}^2}{[D]_{eq}} = \frac{k_{dissoc}}{k_{assoc}} \quad (8)$$

where γ_i is the activity coefficient and is assumed to be unity. Equation 8 may be substituted into eq 7 to yield

$$k_{dissoc} = k_{obs}/[4([D]_{eq}/[M]_{eq}) + 1] \quad (9)$$

Once k_{dissoc} has been determined, k_{assoc} may be calculated from eq 8. The temperature dependence of k_{assoc} and k_{dissoc} may be determined by an Arrhenius plot. The slope of a plot of ln k_{dissoc} vs $1/T$ (K^{-1}) gives $-E_a/R$, where E_a is the activation energy for the dissociation reaction, and R is the gas constant, 1.987 cal mol^{-1} K^{-1}. A similar plot may be constructed for the association reaction to determine the activation energy for that reaction.

RESULTS

Determination of the Aggregate Molecular Mass. Figure 1 shows the size-exclusion chromatograms of rhuMAb VEGF in 10 mM sodium phosphate, pH 7.5, diluted to 1 mg/mL from 30 mg/mL at the intial time point, after 1 h of storage at 40 °C and at equilibrium. Equilibrium was achieved when the concentrations of each peak no longer changed over time. During equilibration at 1 mg/mL, the area of the aggregated species, peak 2, decreased over time while that of the monomer, peak 1, increased. This demonstrated that the rhuMAb VEGF aggregate was dissociable and presumably noncovalent.

To confirm that dissociation of the aggregate did not occur on the HPLC column during analysis, the individual peaks were fraction-collected into a polypropylene tube on ice and reinjected onto the column. The results are displayed in the lower graph in Figure 1. Less than 2% of the total peak area in the fraction containing aggregate can be attributed to monomer, indicating that negligble dissociation occurs during the HPLC analysis. Similarly, the monomer fraction showed no aggregate upon reinjection. This demonstrated that the amounts of monomer and aggregated species were not changing on the HPLC column during analysis.

Initially, the molecular masses of the monomer and the aggregated species were estimated to be 150 kDa and ~410 kDa by a comparison of the SEC retention times of the individual peaks with those of molecular mass standards (Bio-Rad; data not shown). Because the molecular mass of the aggregate roughly corresponded to trimer rather than dimer, multiangle light scattering (MALS) was used to confirm the molecular mass. MALS indicated that, as expected, the molecular mass of the monomer was 150 kDa. However, the molecular mass of the aggregate was 300 kDa, consistent with dimer (data not shown). It is believed that the erroneous result from the SEC molecular mass standard comparison was due to the shape of the dimeric protein resulting in a larger than expected hydrodynamic radius as compared to the proteins used as molecular mass standards.

Effects of Temperature and pH. To investigate the effects of temperature and pH on the rate of dissociation of the rhuMAb VEGF dimer, 30 mg/mL rhuMAb VEGF solutions at pH 8.5, 8.0, 7.5, 7.0, and 6.5, previously incubated at 40 °C for 3 days to expedite dimer formation, were diluted to 1 mg/mL, split into aliquots and stored at 40, 30, and 15 °C. The kinetics of dissociation were assessed by sampling each of these solutions over time to determine the amounts of monomer and dimer present.

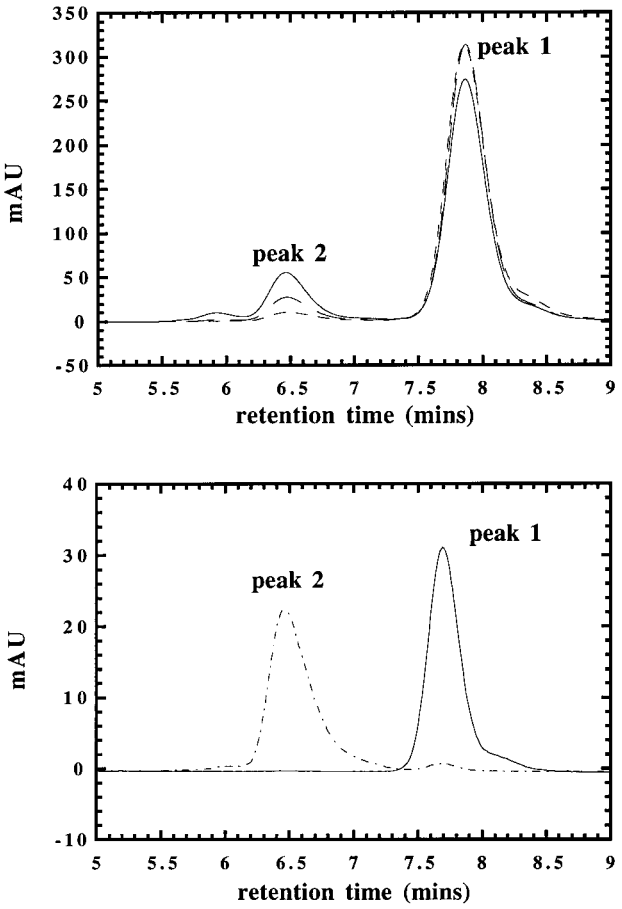

FIGURE 1: Representative SEC chromatograms of rhuMAb VEGF dimer (peak 2) and monomer (peak 1). In the top graph, the displayed data follow the kinetics of reequilibration for a 30 mg/mL rhuMAb VEGF solution at pH 7.5, previously stored at 40 °C to expedite dimer formation at this concentration, after dilution to 1 mg/mL. Data are from the initial timepoint (—), after 1 h of storage at 40 °C (– – –), and at equilibrium at 40 °C (- - -). A small amount of trimer was observed in some experiments. Conditions were used to minimize the amount of trimer present to less than 2% of the total peak area. Because it was often not possible to get good separation between the dimer and trimer, the trimer peak area was included with that of the dimer. The contribution of the trimer area was less than 15% of the total area attributed to dimer. The shoulder following the main peak was included with the main peak area. This shoulder is believed to be a different glycosylated form of the antibody. In the lower graph, fraction-collected dimer (-·-) and monomer (—) were reinjected onto the HPLC column to demonstrate that reequilibration of the rhuMAb VEGF monomer/dimer was not occurring during sample analysis. Less than 2% of the total peak area of the reinjected dimer peak was attributable to monomer, while the reinjected monomer peak showed no evidence of the presence of dimer.

Figure 2 displays the results from this study at 40 °C. The observed rate of dissociation, k_{obs}, was determined using a single-exponential fit of the data points and is presented as the line through the points in Figure 2. The observed rate constant, k_{obs}, for the dissociation reaction decreased approximately 25% with an increase in pH from 6.5 to 8.5 (Table 1). This translated to a similar reduction in k_{dissoc}. These decreases were accompanied by an increase of more than 50% in k_{assoc} as pH was raised from 6.5 to 8.0, followed by a decrease as the pH was further increased to pH 8.5.

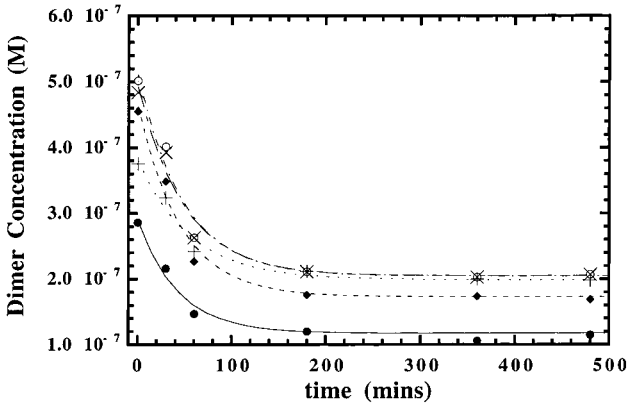

FIGURE 2: The pH dependence of rhuMAb VEGF dimer dissociation. This figure displays the observed kinetics of dimer dissociation at pH 6.5 (filled circle), pH 7.0 (diamond), pH 7.5 (open circle), pH 8.0 (×), and pH 8.5 (+) at 40 °C. The curves through the individual points represent the best fit of the data with a single exponential (see eq 2) to determine k_{obs}. The error between experiments for the determination of k_{obs} was ~25%, although the relative rates did not change.

Table 1: Observed and Calculated Rate Constants for rhuMAb VEGF Dimer Dissociation and Association

temp (°C)	pH	solvent	k_{obs} ($_{min}^{-1}$)[b]	k_{assoc} (M^{-1} min^{-1})[c]	k_{dissoc} (min^{-1})	K_D (M)[d]
40	7.5	10 mM phosphate	0.021	99	0.018	1.8×10^{-4}
30	7.5	10 mM phosphate	0.012	63	0.011	1.8×10^{-4}
15	7.5	10 mM phosphate	0.0045	23	0.0039	1.8×10^{-4}
40	6.5	10 mM phosphate	0.023	61	0.021	3.5×10^{-4}
	7.0	10 mM phosphate	0.022	85	0.020	2.3×10^{-4}
	7.5	10 mM phosphate	0.021	99	0.018	1.8×10^{-4}
	8.0	10 mM phosphate	0.020	105	0.019	1.8×10^{-4}
	8.5	10 mM phosphate	0.018	81	0.016	2.0×10^{-4}
40	7.5	*a*	0.017	81	0.015	1.9×10^{-4}
	7.5	10 mM NaCl	0.021	95	0.018	1.6×10^{-4}
	7.5	100 mM NaCl	0.017	104	0.014	1.4×10^{-4}
	7.5	500 mM NaCl	0.011	86	0.009	1.0×10^{-4}
	7.5	1 M NaCl	0.013	112	0.010	9.1×10^{-5}

[a] The results from the experiment to examine the effects of ionic strength are the average of two experiments, one performed in 10 mM tris, pH 7.5, and the other performed in 10 mM sodium phosphate, pH 7.5. [b] The error in the fit of k_{obs} ranged 5−20%, while the error from repeat experiments was approximately 25%. [c] The error in the determination of k_{assoc} varied between 5 and 23%. [d] The error associated with K_D ranged 2−6%.

Attempts were made to investigate the kinetics of dimer formation and dissociation at pH 5.5, but insignificant levels of dimer formed at this pH even at 30 mg/mL.

Arrhenius plots reveal that there is a linear dependence of ln k_{assoc} and ln k_{dissoc} on inverse temperature at each pH studied. The activation energies determined from the Arrhenius plots for both the association and dissociation reactions range from 9.1 kcal to 11.7 kcal and are displayed in Table 2. At pH 8.0, the activation energy for the dissociation reaction was 1.4 kcal higher than that for the association reaction. At the other pH conditions studied, the activation energy for the dissociation reaction was ≤0.4 kcal higher than that observed for the association reaction. The total amount of dimer present was highly dependent on pH as was reflected in the dissociation equilibrium constants, K_D, displayed in Table 1. At pH 6.5 and 7.0, the differences between activation energies for the association and dissociation reactions were less than 1 kcal/mol, indicating that the monomer and dimer are almost equivalent enthalpically (Table 2). As the pH was increased to pH 8.0, the activation energy for dissociation increases more than that for the association reaction, indicating that the dimerization is enthalpically favored at this pH compared to the others investigated. At pH 8.5, the activation energies for the forward and reverse reactions are again similar. However, because the fit of the data in the Arrhenius plot at pH 8.5 is not as good as the fits at the other pHs, the decreases in the activation energies observed at this pH may not be significantly different to those at pH 8.0.

Table 2: Activation Energies for Dimer Association and Dissociation as a Function of pH

pH	E_a for association (kcal/mol)	E_a for dissociation (kcal/mol)
6.5	9.1	9.3
7.0	10.8	10.8
7.5	10.7	11.1
8.0	10.1	11.5
8.5	11.3	11.7

A more extensive investigation of pH was performed by thermodynamic analysis. A 10 mM sodium phosphate buffer was made at pH 6.5, 7.0, 7.5, 8.0, and 8.5. The equilibrium constants for the various pH buffered solutions are shown in the top graph in Figure 3. The most striking observation is the minimum values of K_D observed in the pH range 7.5−8.5. This indicates that there is an optimal pH for dimer formation. The standard Gibbs' free energy for the dissociation reaction was calculated at each pH (Figure 3, bottom graph) using the following equation:

$$\Delta G^\circ = -RT \ln K_D \tag{10}$$

where R is equal to 1.987 cal/mol K. The maximum free energy at pH 7.5−8.0 confirms that the dimerization reaction is more favorable in this narrow pH range.

The standard enthalpy, ΔH°, for the rhuMAb VEGF dimer dissociation was determined as a function of pH using the van't Hoff equation:

$$\frac{d \ln K_D}{d(1/T)} = \frac{-\Delta H^\circ}{R} \tag{11}$$

and plotting $-\ln K_D$ vs $(1/T)$ with the slope equal to $\Delta H^\circ/R$. The van't Hoff equation was utilized with the assumption that the change in enthalpy, ΔH°, was independent of temperature in the temperature range studied (15−40 °C). The linear relationship observed in Figure 4 confirms this assumption and indicates there is no significant change in the heat capacity. The slopes are slightly positive (0−1.4 kcal/mol), indicating that the reaction is endothermic. The difference in activation energies calculated from Arrhenius plots for association and dissociation reactions are in agreement with the enthalpy values for this reaction reported in Table 3.

Effect of Ionic Strength. The effects of ionic strength on the kinetics of rhuMAb VEGF dimer dissociation were investigated by diluting the 30 mg/mL rhuMAb VEGF solution to 1 mg/mL with either 10 mM Tris or 10 mM sodium phosphate, pH 7.5, containing up to 1 M sodium chloride. The data presented here are the average of the two experiments. As the ionic strength of the medium was

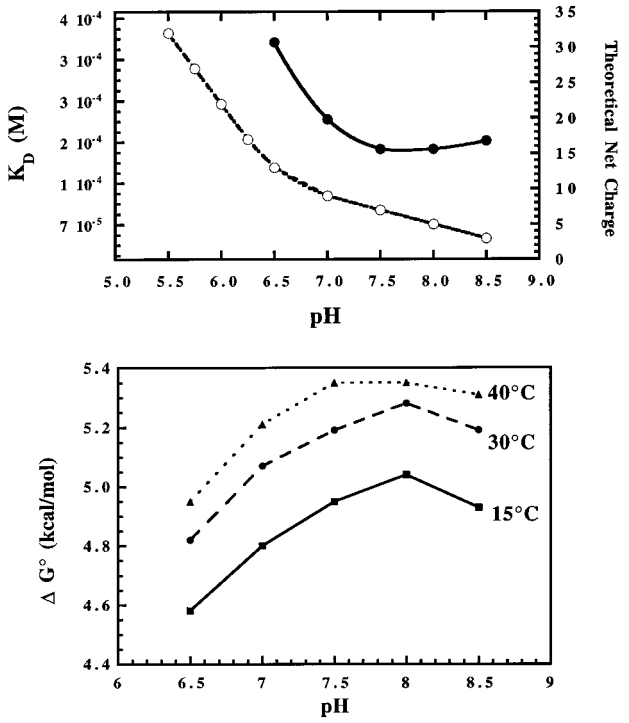

FIGURE 3: Thermodynamic parameters determined as a function of pH and temperature. In the top graph, the K_D (filled circles) and the net charge (open circles) of rhuMAb VEGF at each pH are shown. Samples are 1 mg/mL rhuMAb VEGF and 10 mM sodium phosphate, incubated at 40 °C. The total number of charges on the protein was determined by simple addition of all charged species from the amino acid side chains at each pH, ignoring any contributions from the charges on the carbohydrates. The net charge is the difference in the number of positively charged species and negatively charged species at each pH. The isoelectric point for rhuMAb VEGF was determined to be between 8.2 and 8.3 by isoelectric focusing (data not shown.) This lower experimental value may be reflective of how the protein folds. In the lower graph, a plot of Gibbs' free energy as a function of pH and temperature is displayed. The samples are 1 mg/mL rhuMAb VEGF in 10 mM sodium phosphate incubated at 40 °C (triangles), 30 °C (circles) and 15 °C (squares).

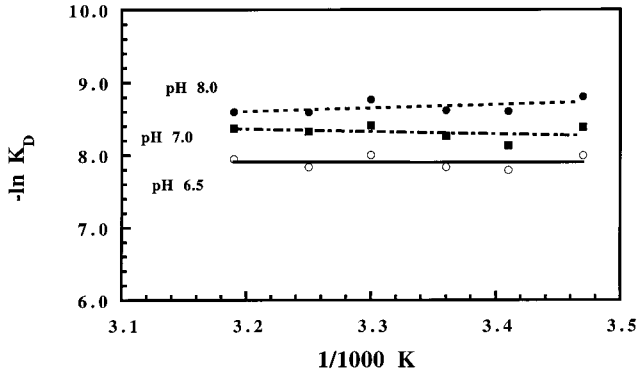

FIGURE 4: van't Hoff plot of $-\ln K_D$ vs $1/T$. The slope, obtained by linear regression, is $\Delta H°/R$. Samples are 1 mg/mL rhuMAb VEGF and 10 mM sodium phosphate, pH 8.0 (filled circles), pH 7.0 (squares), pH 6.5 (open circles).

increased with NaCl, k_{obs} for dimer dissociation decreased as displayed in Figure 5. The overall decrease in k_{obs} resulted from an increase in k_{assoc} and a concurrent decrease in k_{dissoc} (Table 1) at higher ionic strengths.

The effect of ionic strength on the thermodynamics of dissociation of rhuMAb VEGF dimer was studied under three

Table 3: Thermodynamic Parameters for rhuMAb VEGF Dimer Dissociation as a Function of pH[a]

pH	K_D (M)	$\Delta G°$ (kcal/mol)	$\Delta H°$ (kcal/mol)	$T\Delta S°$ (kcal/mol)
6.5	3.5×10^{-4}	4.9	0.4	−4.6
7.0	2.3×10^{-4}	5.2	0.0	−5.2
7.5	1.8×10^{-4}	5.4	0.4	−4.9
8.0	1.8×10^{-4}	5.4	1.3	−4.0
8.5	2.0×10^{-4}	5.3	0.4	−4.9
7.5 + D_2O	1.3×10^{-4}	5.6	ND	ND
7.5 + H_2O	1.8×10^{-4}	5.3	ND	ND

[a] Error is $\leq 1 \times 10^{-5}$ for K_D and ≤ 0.1 for $\Delta G°$, $\Delta H°$, and $\Delta S°$. ND = not determined. Conditions: 1 mg/mL rhuMAb VEGF and 10 mM sodium phosphate, incubated at 40 °C.

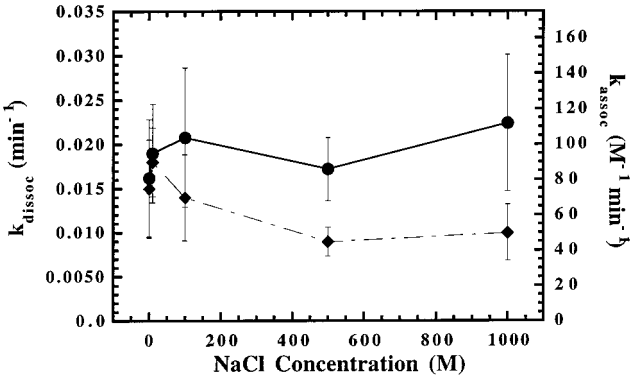

FIGURE 5: Increased ionic strength effects on the rate of rhuMAb VEGF dimer dissociation and association. The rate constants for rhuMAb VEGF dimer dissociation (diamonds) and association (filled circles) were investigated as a function of increasing sodium chloride concentration at pH 7.5. The line connecting the points serves merely as a visual guide. A small effect is observed on both k_{assoc} and k_{dissoc}. The relative lack of sensitivity of these rate constants to ionic strength as compared to other proteins suggests that rhuMAb VEGF self-association does not occur through a specific electrostatic interaction.

Table 4: Thermodynamic Parameters for rhuMAb VEGF Dimer Dissociation as a Function of Ionic Strength[a]

pH	K_D (M)	$\Delta G°$ (kcal/mol)	$\Delta H°$ (kcal/mol)	$T\Delta S°$ (kcal/mol)
6.5	2.6×10^{-4}	5.1	0	−5.1
7.5	8.7×10^{-5}	5.8	0	−5.8
8.5	1.1×10^{-4}	5.7	0	−5.7

[a] Error is $\leq 1 \times 10^{-5}$ for K_D and ≤ 0.1 for $\Delta G°$, $\Delta H°$, and $\Delta S°$. Conditions: 1 mg/mL rhuMAb VEGF and 10 mM sodium phosphate with 1 M NaCl, incubated at 40 °C.

pH conditions. Table 4 lists the thermodynamic parameters calculated for those three systems. In the presence of 1 M NaCl, there was a decrease in the K_D, indicating an increase in ionic strength favored dimer formation. The effect of ionic strength was further studied at pH 7.5 and 40 °C using NaCl and $CaCl_2$ and varying their concentration from 0 to 1 M . The dependence of Gibbs' free energy as a function of ionic strength is plotted in Figure 6. For both salts, an increase in ionic strength favors the dimerization reaction.

The thermodynamic values reported in Tables 3 and 4 fall within the range of values reported for other proteins studied under comparable conditions. The Gibbs' free energy for the dimer dissociation of IgG1-l myeloma protein (IgG-MIT) is 5.1 kcal/mol (*5*) and 5.9 kcal/mol for the dimer dissociation a-chymotrypsin (*1, 2*).

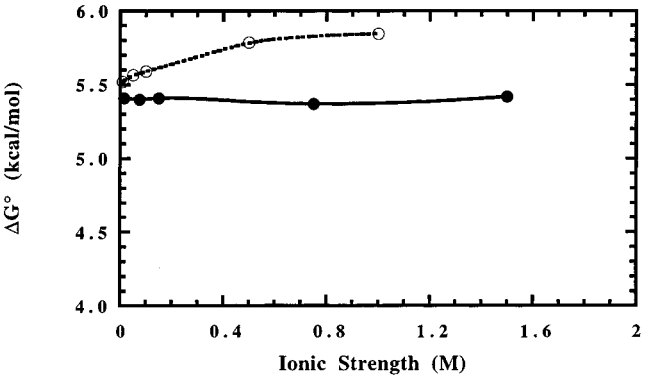

FIGURE 6: Plot of Gibbs' free energy as a function of ionic strength. The rhuMAb VEGF samples are 1 mg/mL in 10 mM Tris, pH 7.5, incubated at 40 °C with added NaCl (open circles) and added $CaCl_2$ (filled circles).

DISCUSSION

During formulation development of rhuMAb VEGF for clinical studies, there was significant self-association of the protein to form dimer and larger oligomers. There are some reports in the literature that monoclonal serum immunoglobulins self-associate (*6*, *14*), and these oligomeric antibodies may contribute to the pathology associated with several disorders including idiopathic cryoglobulinemia (*3*) and rheumatoid arthritis (*4*). Thus, understanding the factors governing the association and dissociation of dimeric antibodies may be critical to formulating a safe therapeutic product.

Although oligomeric antibodies have been implicated in the pathologies of diseases, antibody dimerization is not often observed. For example, trastuzumab, another genetically engineered antibody with the same IgG1 framework and 92% sequence homology to rhuMAb VEGF (*11*, *15*), does not form a significant amount of aggregate under identical conditions (data not shown). The reversible self-association of rhuMAB VEGF is an uncommon phenomenon for an IgG1 antibody, although it is a distinguishing feature of antibodies of the IgG3 isotype (*6*).

In addition to the unique formation of a homodimer, the self-association of the rhuMAb VEGF was found to be much slower than that observed for other proteins, even those much larger than rhuMAb VEGF. A partial listing of rate constants for protein self-association from the literature is presented in Table 5. In the experiment reported here, the rate constant for rhuMAb VEGF association was found to range between 23 and 112 M^{-1} min^{-1} under the various conditions studied. These rates are more than fifty times slower than the rate of self-association of phosphorylase b dimer (240 kDa) to form tetramer (*16*). While the rate of association of the rhuMAb VEGF dimer is much slower than observed for other proteins, the rate of dissociation, k_{dissoc}, is within the range of rates reported. As displayed in Table 5, the rates of dissociation vary greater than 6 orders of magnitude between proteins listed and even vary extensively for one protein under different conditions. For example, k_{dissoc} for stem cell factor increased more than 100-fold when the pH of the solution was decreased from 8.2 to 3.2 (*17*). The k_{dissoc} for rhuMAb VEGF dimer varied from 0.0039 to 0.021 min^{-1}. An advantage of these slow kinetics is the ability to study this system using size-exclusion chromatography, because both association and dissociation of the rhuMAb VEGF dimer occur over a slower time scale than used by the chromatographic method.

Table 5: Reported Rates of Association and Dissociation for Protein Self-Association

protein	reaction[a]	k_{assoc} (M^{-1} min^{-1})	k_{dissoc} (min^{-1})	temp (°C)	conditions
platelet factor 4[b]	2M ↔ D	8×10^6	2100	30	
phosphorylase b[c]	2D ↔ T	6×10^3	0.63	28.5	pH 6.9
		7×10^3	0.42	25	pH 6.9
		6×10^3	0.10	20	pH 6.9
		6×10^3	0.063	16	pH 6.9
stem cell factor[d]	2M ↔ D		1.54	37	pH 3.2
			0.054	37	pH 4.5
			0.068	37	pH 4.5, 1 M NaCl
			0.0032	37	pH 8.2
hexokinase PI[e]	2M ↔ D	7×10^6	12.6	20	pH 8.0, 0.1 M KCl
HIV protease subunits[f]	2M ↔ D	2×10^7	1.5	37	pH 7.5
		4×10^7	0.20	37	pH 6.0
growth hormone[g]	2M ↔ D	1×10^6	1.25	25	pH 7.5, 0.1 M NaCl

[a] M = monomer, D = dimer, T = tetramer; data have been converted to the appropriate units where necessary. [b] Data from ref *27*, results in the presence of 0.1 mM AMP. [c] Data from ref *16*. [d] Data from ref *17*. [e] Data from ref *28*, in the absence of glucose. [f] Data from ref *29*. [g] Data from ref *30*.

From the slow kinetics of rhuMAb VEGF self-association, it may be concluded that the association is not diffusion-limited. This indicates there are additional variables besides diffusion governing the rate of rhuMAb VEGF self-association. These variables may include such factors as the pH and the ionic strength of the medium, which could serve to enhance specific protein−protein interactions. Interactions that drive protein self-association include hydrophobic interactions, ionic interactions, or a combination of the two. Information obtained from a kinetic and a thermodynamic analysis of the factors governing dimerization may be used to elucidate the type of interaction responsible for protein self-association.

Thermodynamic analysis of rhuMAB VEGF dissociation suggests that there is a hydrophobic interaction responsible for self-association. The enthalpy is near zero for the dissociation of rhuMAb VEGF, indicating that the self-association must be entropically driven. The standard entropy, $\Delta S°$, was calculated from

$$\Delta G° = \Delta H° - T\Delta S° \qquad (12)$$

for the various conditions and is listed in Tables 3 and 4. The dissociation of dimer to monomer results in a decrease in entropy, which is indicative of a hydrophobic interaction. As dimer dissociates to monomer, water molecules must order themselves around the exposed hydrophobic side chains of the monomer thus decreasing entropy (*2*).

To support the existence of a hydrophobic effect, the dissociation equilibrium constant was determined in the presence of deuterium oxide (D_2O). It has been proposed that hydrophobic interactions are stronger in the presence of D_2O (*18*). If the dimerization of rhuMAb VEGF is the result of a hydrophobic interaction, then it will be favored in the presence of D_2O. Samples of rhuMAb VEGF at 30

mg/mL were diluted to 1 mg/mL in either D_2O or H_2O, and the dissociation equilibrium constant at 40 °C was determined. No insoluble aggregates were observed as a result of the addition of D_2O. As seen in Table 3, dimerization was enhanced in the presence of D_2O. The lower K_D observed for rhuMAb VEGF in D_2O supports the idea that, as dimer forms, water is excluded from the hydrophobic side chains of the monomer. Similar results were observed for the dimerization of α-chymotrypsin, a protein that has been shown to self-associate partly due to a hydrophobic effect (*1*, *2*).

There are other immunoglobulins that self-associate due to hydrophobic effects, such as IgG-MIT(*5*). The self-association of IgG-MIT was determined to be enthalpically driven, whereas the dimer formation of rhuMAb VEGF is entropically favored. These differences suggest that there are other interactions, along with hydrophobicity, that are involved in self-association of rhuMAb VEGF.

In addition to the hydrophobic interaction, the rhuMAb VEGF monomers could interact via electrostatic interactions. Electrostatic interactions have been shown to be involved in the self-association of stem cell factor (*17*), as well as α-chymotrypsin (*1*, *2*) and platelet factor 4 (*19*). Unlike the specific anionic−cationic interaction that forms the α-chymotrypsin dimer (*1*, *2*), the dependence of rhuMAb VEGF dimerization on pH correlates with the pI of the protein. This can been seen in the top graph in Figure 3 where the theoretical net charge is plotted as a function of pH. This value was calculated from the contribution of all the amino acids (*20*) and ignores any contribution from carbohydrates. The top graph in Figure 3 demonstrates that the K_D is at a minimum when the net charge is near zero. The decrease in net charge and thus a decrease in repulsive forces may allow the dimer to form.

This assumption is supported from the kinetic analysis in which the rate constant for association at pH 6.5 was only 60% of that observed at pH 7.5 and 8.0. Because this difference occurs over a fairly narrow pH range, it is unlikely due to a conformational effect of the protein because there are only a few residues that will have a change in ionization over this range. Ionizable groups with pK_a values in the range 6.5−9.0 include histidine and terminal amino groups (*21*). Cysteine also has an ionizable group in this pH range, but there are no free thiols in rhuMAb VEGF.

As with the pH effect, there was a relatively small ionic strength effect on the rate of rhuMAb VEGF dimer formation, with k_{assoc} increasing only ∼20% as the ionic strength of the solution was increased with the addition of 1 M NaCl. The tendency to form more dimer at high ionic strengths (Table 1) suggests that the dimer formation is not due to a specific ionic interaction. These results are consistent with the pH data and imply that charge shielding, which results in a decrease in the repulsive forces, leads to an increase in the rate of dimerization.

The self-association of some proteins has been shown to depend largely on pH and ionic strength. In the case of stem cell factor, the k_{dissoc} was shown to be highly dependent on the pH of the solution, leading the authors to conclude that the association of the monomers occurred through electrostatic interactions at the monomer−monomer interface (*17*). With platelet factor 4, the amount of dimer was significantly affected by pH and by the ionic strength, leading to the conclusion by Mayo and Chen that dimer formation in this system resulted from an intermolecular salt bridge between Glu28 and Lys50 (*19*). In this study, there was relatively little variability in the k_{dissoc} for rhuMAb VEGF dimer dissociation under all of the conditions studied (Table 1). The effects of pH and ionic strength on the rate of dimer dissociation were modest, with only a 25% difference observed over the pH range and sodium chloride range studied. By comparison, the effects of temperature on the rate of dissociation showed a greater than 4-fold decrease at pH 7.5 when the temperature was decreased from 40 to 15 °C, with similar results observed at other pHs. These results are in marked contrast to those observed for stem cell factor and platelet factor 4. The lack of sensitivity of the rhuMAb VEGF dimer dissociation on the ionic strength and pH of the solution suggests that electrostatic interactions are not the predominant source of the interactions leading to dimerization. The increase in the amount of dimer in the presence of 1 M NaCl also indicates that hydrophobic interactions may contribute to rhuMAb VEGF dimerization and that there are no specific ionic interactions leading to self-association.

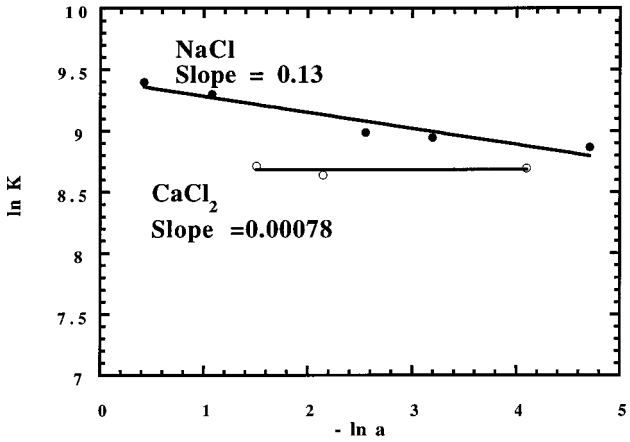

FIGURE 7: A plot of ln K_D vs −ln *a*. The rhuMAb VEGF samples are 1 mg/mL in 10 mM Tris, pH 7.5, incubated at 40 °C with added NaCl (open circles) and added $CaCl_2$ (filled circles). The ion pair activity was estimated using the mean activity coefficients for $CaCl_2$ and NaCl at 25 °C (*31*).

A thermodynamic analysis of the data supports the supposition that there are no specific ionic interactions contributing to the self-association of rhuMAb VEGF. The theory of linked functions (*22*) was used to determine if the dimer enhancement was due to an ionic interaction. In Figure 7, the logarithm of the dissociation equilibruim constant was plotted against the logarithm of the ion-pair activity (*a*). The relationship is linear, and using the equations worked out by Wyman (*22*), Tanford (*23*), and Aune and Timasheff (*1*, *2*), the slope of the line is determined to be $\Delta\upsilon_{pref}$

$$\frac{(\partial \ln K)}{(\partial \ln a)} = \Delta\upsilon_{pref} \qquad (13)$$

The quantity $\Delta\upsilon_{pref}$ is the difference between the preferential binding of solvent components to monomer and dimer.

In Figure 7, $\Delta\upsilon_{pref}$ is 0.13 for NaCl and 0.001 for $CaCl_2$. These values are small compared to other proteins that self-associate under ionic conditions, such as α-chymotrypsin where $\Delta\upsilon_{pref}$ is 1.06 for NaCl. Since $\Delta\upsilon_{pref}$ is substantially less than 1 for both NaCl and $CaCl_2$, no ion binding is

occurring during rhuMAb VEGF dimer formation, and there are no ion-specific interactions resulting in the formation of rhuMAb VEGF dimer.

The study reported here determined that rhuMAb VEGF monomer self-association is the result of a hydrophobic interaction, although there does appear to be a small electrostatic contribution as determined by the sensitivity of self-association to the pH of the solution. It has been proposed that the interactions leading to self-association of monoclonal antibodies occur in the unique sequences in the variable region of the antibody (*24*), although there is relatively little literature concerning this topic. By definition, the hypervariable regions of antibodies show the greatest differences in sequences between different antibodies of the same class. Thus, involvement of the Fab in self-association of rhuMAb VEGF would not be unexpected. Preliminary competition experiments comparing the binding of VEGF to the rhuMAb VEGF monomer and to the rhuMAb VEGF dimer imply that the Fab region of the antibody is near the binding interface of the dimer, because VEGF bound predominantly to the monomer form (data not shown.)

If the Fab of rhuMAb VEGF is proven to be involved in dimer formation, its participation does not exclude the involvement of other regions of the antibody in dimerization. Studies of bovine immunoglobulin G1 showed that removal of the Fc portion of the protein by pepsin removed its ability to self-associate (*25*). Protein MAT, a human IgM cryoprecipitating cold agglutinin, self-associates via an interaction between the Fab region and a carbohydrate moiety on the Fc portion of the protein (*26*). Studies of murine IgG3 reported that glycosylation in the Fc portion was influential in the self-association of the antibody (*6*). The involvement of the Fc region in rhuMAB VEGF dimerization could be further studied using other antibodies that contain identical Fc regions to rhuMAb VEGF, namely trastuzumab. Investigation of the participation of these regions and the specific interactions leading to rhuMAb VEGF dimerization are currently under investigation in our laboratory.

ACKNOWLEDGMENT

The authors wish to thank Niyana Barron-Avilez and Jun Liu for the technical support.

REFERENCES

1. Aune, K. C., and Timasheff, S. N. (1971) *Biochemistry 10*, 1609−1616.
2. Aune, K. C., Goldsmith, L. C., and Timasheff, S. N. (1971) *Biochemistry 10*, 1617−1622.
3. Pope, R. M., Mannik, M. M., Gilliland, B. C., and Teller, D. C. (1975) *Arthritis Rheum. 18*, 97−106.
4. Brouet, J. D., Clauvel, J. P., Danon, F., Klein, M., and Seligman, M. (1975) *Am. J. Med. 57*, 775−788.
5. Hall, C. G., and Abraham, G. N. (1984) *Biochemistry 23*, 5123−5129.
6. Panka, D. J. (1997) *Mol. Immunol. 34* (8/9), 593−598.
7. Kim, K. J., Li, B., Winer, J., Armanini, M., Gillett, N., Phillips, H. S., and Ferrara, N. (1993) *Science 362*, 841−844.
8. Börgstrom, P., Hillan, K. J., Sriramarao, P., and Ferrara, N. (1996) *Cancer Res. 56*, 4032−4039.
9. Börgstrom, P., Bourdon, M. A., Hillan, K. J. Sriramarao, and Ferrara, N. (1998) *Prostate 35* (1), 1−10.
10. Pham, C. D., Roberts, T. P. L., van Bruggen, N., Melynk, O., Mann, J., Ferrara, N., Cohen, R. L., and Brasch, R. C. (1998) *Cancer Invest. 16* (4), 225−230.
11. Presta, L. G., Chen, H., O′Connor, S. J., Chisholm, V., Meng, Y. G., Krummen, L., Winkler, M., and Ferrara, N. (1997) *Cancer Res. 57*, 4593−4599.
12. Zimm, B. H. (1948) *J. Chem. Phys. 16*, 1093−1099.
13. Espenson, J. H. (1981) Kinetics of Complex Reactions - - Reversible and Concurrent Reactions. *Chemical Kinetics and Reaction Mechanisms*, pp 48−50, McGraw-Hill Series in Advanced Chemistry, McGraw-HIll Book Company.
14. Middaugh, C. R., and Litman, G. W. (1987) *J. Biol. Chem. 262* (*8*), 3671−3673.
15. Carter, P., Presta, L., Gorman, C. M., Ridgway, J. B. B., Henner, D., Wong, W. L. T., Rowland, A. M., Kotts, C., Carver, M. E., and Shepard, H. M. (1992) *Proc. Natl. Acad. Sci. U.S.A. 89*, 4285−4289.
16. Muñoz, F., Valles, M. A., Donoso, J., Echevarria, G., and Garcia Blanco, F. (1983) *J. Biochem. 94*, 1649−1659.
17. Lu, H. S., Chang, W.-C., Mendiaz, E. A., Mann, M. B., Langley, K. E., and Hsu, Y.-R. (1995) *Biochem. J. 305*, 563−568.
18. Kresheck, G. C., Schneider, H., and Scheraga, H. A. (1965) *J. Phys. Chem. 69* (9), 3132−3144.
19. Mayo, K. H., and Chen, M.-J. (1989) *Biochemistry 28*, 9469−9478.
20. Lehninger, A. L. (1976) *The Amino Acid Building Blocks of Proteins: Biochemistry*, p 79, Worth Publishers, Inc., New York.
21. Stryer, L. (1988) *Protein Structure and Function: Biochemistry*, p 21, W. H. Freeman and Company, New York.
22. Wyman, J. (1964) *Adv. Protein Chem. 19*, 224.
23. Tanford, C. (1969) *J. Mol. Biol. 39*, 539−544.
24. Erickson, B. W., Gerber-Jenson, B., Wang, A.-C., and Litman, G. W. (1982) *Mol. Immunol. 19* (*3*), 357−365.
25. Mukkur, T. K. S., and Smith, G. D. (1979) *Biochem. J. 183*, 463−465.
26. Weber, R. J., Clem, L. W., and Voss, E. W., Jr. (1984) *Mol. Immunol. 21* (1), 61−67.
27. Chen, M.-J., and Mayo, K. H. (1991) *Biochemistry 30*, 6402−6411.
28. Hoggett, J. G., and Kellett, G. L. (1992) *Biochem. J. 287*, 567−572.
29. Darke, P. L., Jordan, S. P., Hall, D. L., Zugay, J. A., Shafer, J. A., and Kuo, L. C. (1994) *Biochemistry 33*, 98−105.
30. Patapoff, T. W., Mrsny, R. J., and Lee, W. A. (1993) *Anal. Biochem. 212*, 71−78.
31. Lide, D. R. (1994) *CRC Handbook of Chemistry and Physics*, *75th ed.*, pp 5-94−5-95, CRC Press, Boca Raton, FL.

BI9905516